Differences in the Solution Structures of Oxidized and Reduced Cytochrome *c* Measured by Small-Angle X-ray Scattering†

Jill Trewhella,* Vanice A. P. Carlson, Elizabeth H. Curtis, and Douglas B. Heidorn

Life Sciences Division and Neutron Scattering Center, Los Alamos National Laboratory, Los Alamos, New Mexico 87545

Received June 25, 1987; Revised Manuscript Received September 22, 1987

ABSTRACT: While X-ray crystallographic data on cytochrome *c* show the reduced and oxidized forms to have very similar structures, there is a considerable body of data, mostly from solution studies, that indicates the reduced form is more stable and that the interior of the protein is less accessible to solvent in this state. These observations have led to the hypothesis that while the time-averaged structure is preserved between the two forms, the dynamics of the two forms are different. The oxidized form has been proposed to undergo more large-amplitude, low-frequency motions than the reduced form. The crystal structure data were derived from crystals grown in high salt concentrations, but the solution studies were done at relatively low ionic strength. Small-angle X-ray scattering has been used to examine the effects of the ionic strength and oxidation state on the solution structure of cytochrome *c*. We find that the radius of gyration and the maximum linear dimension of oxidized cytochrome *c* are significantly larger than those for reduced cytochrome *c*, in 5 mM phosphate buffer at pH 7.3, and further that this difference is suppressed by addition of 200 mM sodium chloride. We conclude that there is a real structural difference between the two forms at low ionic strength in solution and that this difference is likely to contribute to the observed differences in accessibility and compressibility.

Cytochromes *c* are small heme-containing proteins that function in the electron-transport systems of prokaryotic and eukaryotic cells (Margoliash & Schejter, 1966). They may exist in an oxidized (ferric) or reduced (ferrous) state. Reversible conversion between the two states in vivo is brought about by interactions with cytochrome oxidase or cytochrome reductase. The precise mechanism by which the electron transfer is achieved, however, is not known.

Spectroscopic data show that there are dramatic differences in the hydrogen exchange rates between oxidized and reduced cytochrome *c*. Increases of more than an order of magnitude in hydrogen exchange rates have been observed on going from the reduced ferrous to the oxidized ferric state by infrared (Ulmer & Kagi, 1968; Kagi & Ulmer, 1968) and NMR (Patel & Canuel, 1976; Wand et al., 1986) spectroscopy. In addition, physical chemical studies on denaturation have shown that reduced cytochrome *c* is substantially more stable than the oxidized form (Margoliash & Schejter, 1966). These results were in apparent conflict with high-resolution crystallographic data on cytochrome *c* that show the crystal structures of the two forms to be very similar (Takano & Dickerson, 1981). The similarity of the two structures is also supported by extended X-ray absorption spectra (EXAFS) that indicate there is no change in the coordination geometry of the heme on oxidation (Labhardt & Yuen, 1979).

Eden and co-workers (Eden et al., 1982) measured densities and sound velocities in cytochrome *c* solutions and concluded that there is a 40% increase in apparent compressibility of cytochrome *c* on oxidation. This result was interpreted as indicating there is an increase in the root-mean-square volume fluctuation δV_{rms} in the oxidized form [$\delta V_{rms}(ox)/\delta V_{rms}(red)$ was estimated as 96 Å^3/74 Å^3]. This conclusion was supported by the observation that the crystallographic thermal parameters, which are most sensitive to large-amplitude, low-frequency collective motions, are uniformly larger for oxidized cytochrome *c* than those for the reduced form. More recently, Kharakoz and Mkhitaryan (1986) have published compressibility studies on cytochrome *c* from which they conclude that the increase in apparent compressibility is only 2% on oxidation. They contend that this result concurs with their hypothesis that changes in protein compressibility are small in processes not accompanied by large structural rearrangements.

On the basis of their own compressibility studies, combined with the high-resolution structural data and the various spectroscopic studies, Eden and co-workers (Eden et al., 1982) proposed that while the time-averaged structures of oxidized and reduced cytochrome *c* are the same, their dynamics are different, in that the oxidized form undergoes more low-frequency, large-amplitude motions than the reduced form. Such a difference in dynamic behavior could account for the different hydrogen exchange behavior, the compressibility results, and the observations concerning the relative stability of the two forms. It has been further suggested that this proposed difference in the dynamics might be important in the regulation of electron transport.

The crystal structure data on cytochrome *c* were derived from crystals grown in high salt concentrations, while the spectroscopic data and compressibility studies were all done in relatively low salt concentrations. In view of this, we decided to measure X-ray scattering data on oxidized and reduced cytochrome *c* in solutions of different ionic strength to see if there were any effects on the structure. If so, then it might not be necessary to invoke differences in dynamic behavior in the absence of changes in time-averaged structure in order to explain the spectroscopic and compressibility data. We find that for the solution conditions used in the compressibility studies (i.e., 5 mM phosphate buffer, pH near 7) there is a real structural difference between oxidized and reduced cytochrome *c*. This difference is suppressed when the ionic strength of the solution is increased by addition of sodium

† This work is supported by the Department of Energy, Office of Health and Environmental Research, Project HA-02-02-03/B04664.

* Author to whom correspondence should be addressed.

0006-2960/88/0427-1121$01.50/0

chloride. We conclude that the structural difference is not seen in the crystallographic data because of the high ionic strength environment of the crystals. Further, the structural differences observed in the solution studies are likely to contribute to the different hydrogen exchange and compressibility results for the two forms.

Materials and Methods

Sample Preparation. Horse heart cytochrome *c* was purchased from Sigma and used without further purification. All samples were buffered in 5 mM sodium phosphate at pH 7.3 with 0.02 mM ethylenediaminetetraacetic acid (EDTA) (buffer A). The "high" salt samples also contained 200 mM NaCl. The EDTA was used to inhibit autoxidation of the reduced form. Fully oxidized samples were prepared by dissolving cytochrome *c* in a solution containing an excess of ferricyanide (buffered at pH 7.3 with 50 mM phosphate) and then passing this solution down a Sephadex G-25 medium column equilibrated with buffer A. Reduced samples were prepared by passing the cytochrome *c* through a band of sodium dithionite on a Sephadex G-25 fine column equilibrated with buffer A. The purity of the final oxidation state was determined by monitoring the visible absorption spectrum in the region 500–600 nm (Margoliash & Frowirth, 1959). Oxidized samples were fully oxidized. Reduced samples were found to stay better than 90% reduced for the duration of the experiment. Concentrations were also determined spectrophotometrically. For a given dilution series, the dilutions were done gravimetrically, and protein concentrations and oxidation state were rechecked by the absorption spectrum after the X-ray measurement.

X-ray Scattering Measurements. X-ray data were collected on a small-angle X-ray scattering station at Los Alamos. This station uses a line from a sealed-tube X-ray source driven by an Enraf Nonius generator operated between 1.2 and 1.5 kW; 8.5-keV X-rays from a copper anode pass through a nickel filter and are focused, by reflection from a glass mirror, at the plane of a Tennelec 100 one-dimensional position sensitive detector. The samples for measurement were positioned behind guard slits (to remove parasitic scattering) halfway between the mirror and the detector. The sample was centrifuged into a 1-mm quartz capillary that was glued into a brass holder. The sample holder was maintained at a constant temperature (23 °C) by circulating water. The sample-to-detector distance was 33 cm. Data were recorded on an IBM PC installed with a Nucleus PCA-8000 multichannel analyzer board. The response of the position-sensitive detector was checked for uniformity before and after each set of experiments. Backscatter from a lead beam-stop was used to monitor the transmitted beam intensity, and this was used to normalize the intensity data. The net scattering from the protein molecules alone was calculated by subtracting a normalized buffer spectrum measured in the same sample cell. By use of the partial specific volume of the protein, a correction was made for the volume occupied by the protein molecules in the protein solution. Typical data collection times were 2–12 h, depending on the protein concentrations.

Remeasurement of the scattering for samples showed no changes in the derived $P(r)$ functions, nor the R_g values. In addition, no changes were observed in the sodium dodecyl sulfate gel electrophoretic bands after X-ray irradiation. X-ray damage was, therefore, assumed to be minimal.

Scattering Data Analysis. Data were summed from detector channels at scattering angles of equal magnitude on opposite sides of the direct beam for all analyses. Data that had been corrected for slit smearing (Moore, 1980) were analyzed with the Guinier approximation (Guinier, 1939) as well as with an indirect Fourier transform analysis of Moore (1980).

The Guinier approximation says that, for scattering from a point source by a homogeneous solution of monodisperse particles, at sufficiently small scattering angles a plot of ln I versus $(2\theta)^2$ will be linear, with a slope that is related to the radius of gyration R_g by

$$R_g^2 = \frac{3\lambda^2}{4\pi^2} \frac{\Delta \ln I(2\theta)}{\Delta(2\theta)^2}$$

where I is the scattered intensity, 2θ is the scattering angle, and λ is the wavelength of the scattering radiation (1.54 Å for Cu Kα). R_g values were calculated from the straight line fit of the scattering data that satisfied the condition $R_g q_{max} \leq 1.3$, where $q = 4\pi(\sin\theta)/\lambda$. Statistical errors were propagated from the counting statistics in the fitting procedure, which also gave the net scattered intensity at zero angle, I_0, and its error.

For the Moore analysis data were used out to $q^2 = 0.08$ Å^{-2}, and the length distribution functions $P(r)$ were calculated directly from the scattering intensity by a Fourier inversion:

$$P(r) = \frac{1}{2\pi^2} \int_0^\infty I(q) qr[\sin(qr)]\, dq$$

The length distribution is simply the frequency of vectors connecting small-volume elements within the entire volume of the scattering particle. Beyond a distance d_{max}, the maximum linear dimension of the particle, the $P(r)$ function vanishes. The radius of gyration may also be computed from the second moment of the $P(r)$:

$$R_g^2 = \frac{\int_0^{d_{max}} P(r) r^2\, dr}{2\int_0^{d_{max}} P(r)\, dr}$$

Length distributions were calculated for a range of d_{max} values. Typically, the computed reduced χ^2 values for the calculated and experimental intensities decreased from values much greater than 1 for small d_{max} to a stable minimum, and the computed R_g reached a plateau as d_{max} was increased. At significantly larger values of d_{max} the $P(r)$ function gave negative values. The final d_{max} was chosen according to the criteria of Glatter (Glatter, 1982), and the corresponding R_g value thus derived was checked for agreement with that determined by the Guinier analysis of data that had been corrected for slit smearing.

Effects of interparticle interference on the computed R_g values from both the $P(r)$ and Guinier analyses were corrected by a least-squares linear extrapolation of plots of R_g^2 versus protein concentration to zero protein concentration (Zaccai & Jacrot, 1983). The experimental $P(r)$ functions were also calculated by extrapolation to zero protein concentration (Moore, 1980).

Model Calculations. $P(r)$ functions were calculated from models based on the α-carbon coordinates derived from the crystal structure analysis (Takano & Dickerson, 1981) with a Monte Carlo integration technique. Homogeneous spheres representing each amino acid were positioned according to the α-carbon coordinates; the size and X-ray scattering power of each sphere are estimated from the partial specific volume and chemical composition of the amino acid it represents. The model structure is then placed in a box, such that it is wholly contained within the box. The Monte Carlo routine generates random points within the box, and if the point is also contained within the model, it is saved. Distances between every pair

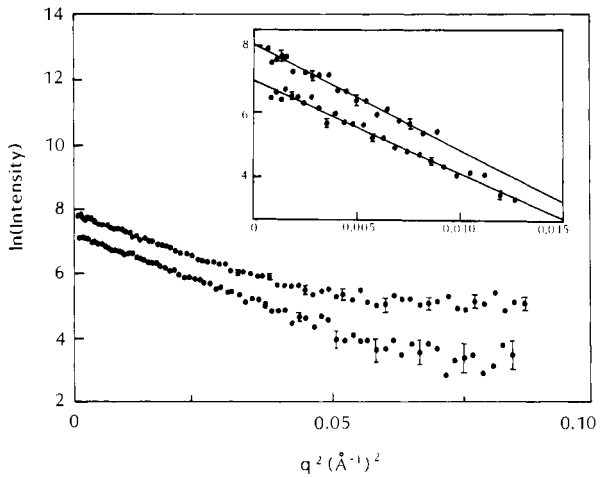

FIGURE 1: Extended scattering curves for oxidized (upper) and reduced (lower) cytochrome *c*, at 11.7 and 9.9 mg/mL, respectively. The inset shows the corresponding Guinier regions.

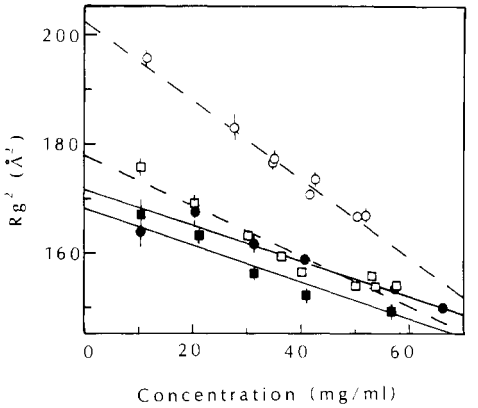

FIGURE 2: Concentration dependence of the R_g values determined with the $P(r)$ analysis for oxidized cytochrome *c* at (○) 0 and (●) 200 mM NaCl and for reduced cytochrome *c* at (□) 0 and (■) 200 mM NaCl.

of saved points are binned and weighted according to the product of the electron scattering powers at each point. The resulting histogram is the calculated $P(r)$ function. For model calculations involving the effects of the disposition of side chains at the surface of the structure, smaller spheres, representing individual atoms and positioned according to the crystal structure coordinates, were used. Side-chain orientations for these latter calculations were manipulated at a Silicon Graphics IRIS workstation with MIDAS (Computer Graphic Laboratory, University of California, San Francisco) installed.

Results

Figure 1 shows extended scattering curves for oxidized cytochrome *c* at 0 mM NaCl, as well as reduced cytochrome *c* at 0 mM NaCl. In each case the protein concentrations are approximately 10 mg/mL. This was the lowest protein concentration measured, and the errors shown are therefore the largest for any of the measured data. The Guinier regions for each curve are shown in the inset. Note, there is no evidence for upward curvature at low angle in the scattering data that would result from aggregation of the protein. Plots of I_0/c versus *c*, where *c* is the protein concentration, for a given set of sample conditions, were linear and also showed no evidence for aggregation. Values of I_0 obtained for each sample condition on extrapolation to zero concentration were the same within experimental error, as is expected for scattering from molecules of approximately equivalent molecular weight

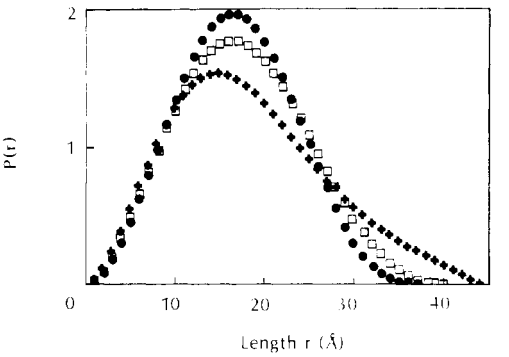

FIGURE 3: $P(r)$ functions calculated for oxidized cytochrome *c* at (+) 0 and (●) 200 mM NaCl and for reduced cytochrome *c* at (□) 0 mM NaCl. In each case the intensity data were extrapolated to infinite dilution for the calculation. The size of the symbols is equal to the largest error in $P(r)$.

Table I: R_g and d_{max} Values of Cytochrome *c* Determined for Infinite Dilution[a]

	0 mM NaCl		200 mM NaCl	
	R_g (Å)	d_{max} (Å)	R_g (Å)	d_{max} (Å)
oxidized				
$P(r)$	14.2 ± 0.2	44 ± 2	13.1 ± 0.2	37 ± 2
Guinier	14.2 ± 0.4		13.3 ± 0.5	
reduced				
$P(r)$	13.3 ± 0.2	40 ± 2	13.0 ± 0.3	39 ± 2
Guinier	13.6 ± 0.4		13.2 ± 0.4	

[a] Crystal structure values: (oxidized) R_g = 12.93 Å and d_{max} = 39.22 Å; (reduced) R_g = 12.96 Å and d_{max} = 39.40 Å.

(Kringbaum & Kugler, 1970).

Figure 2 shows the concentration dependence of the R_g^2 values calculated from the $P(r)$ analysis for both oxidized and reduced cytochrome *c*, each with 0 and 200 mM NaCl. The linear dependence of R_g^2 with concentration is expected from interparticle interference effects and again indicates there is no protein aggregation over the concentration range examined. $P(r)$ functions computed for infinite dilution for oxidized cytochrome *c* at 0 and 200 mM NaCl as well as reduced cytochrome *c* at 0 mM NaCl are shown in Figure 3. The largest errors in the $P(r)$ curves are represented by the size of the symbols. The $P(r)$ function determined for reduced cytochrome *c* at 200 mM NaCl is omitted because it is not significantly different from that determined at 0 mM NaCl. Table I summarizes the R_g and d_{max} values measured for each sample condition with both the Guinier and the $P(r)$ analyses.

The data shown were reproducible; each set of conditions was measured two or three times with independent sample preparations, yielding the same results. Comparisons of each sample condition were initially made between sets of data collected for identical scattering geometry, with the same sample cell, over a period of time for which there was no significant change in the detector sensitivity, etc. It was found, however, that providing the scattering geometry was preserved there were no systematic differences between independent dilution series for the same sample conditions.

From Table I it is evident that the radius of gyration increases (by approximately 7%) on going from the reduced to the oxidized state in the low ionic strength conditions. This result is independent of whether the R_g values are obtained by Guinier analysis or from the $P(r)$ analysis, though the errors are larger for the Guinier analysis, since fewer data contribute in this case. There is a corresponding increase in the maximum vector length (from 40 to 44 Å). These changes in parameters are reflected by a general redistribution of vectors in the $P(r)$ function such that there are significantly more vectors greater

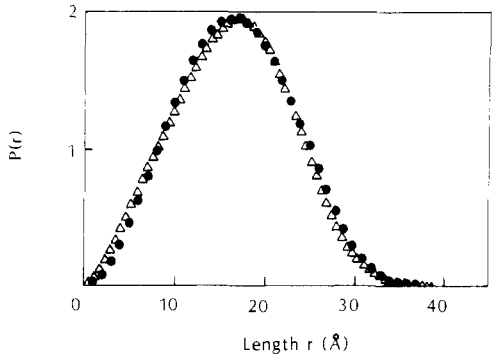

FIGURE 4: $P(r)$ functions calculated for oxidized cytochrome c on the basis of the crystal structure (△) and from the experimental data at 200 mM NaCl (●), extrapolated to infinite dilution. The size of the symbols is equal to the largest errors in $P(r)$ calculated for the experimental data.

than approximately 30 Å for oxidized cytochrome c and correspondingly fewer shorter vectors.

The radius of gyration for oxidized cytochrome c decreases with increasing ionic strength. There is an 8% reduction in R_g on going from 0 to 200 mM NaCl and a corresponding decrease in the maximum vector length (44 to 37 Å). The redistribution in the $P(r)$ function is similar to that observed between oxidized and reduced cytochrome c at low ionic strength. Generally there are fewer vectors longer than 30 Å and more shorter vectors in the high-salt condition.

The difference in R_g observed for reduced cytochrome c between 0 and 200 mM NaCl, is at the limit of what is detectable by these techniques (2 ± 2%) and may not be significant, and there is no significant change in the $P(r)$ function. There is no measurable difference in the R_g values between oxidized and reduced cytochrome c in 200 mM NaCl.

Figure 4 shows a comparison of the experimental $P(r)$ functions calculated for oxidized cytochrome c in 200 mM NaCl with that calculated from the crystal structure coordinates (Brookhaven Data Bank coordinates; Takano & Dickerson, 1981). The crystal structure data agree very well with the high salt solution data but show significant differences with the low salt solution data. The R_g and d_{max} values calculated for the $P(r)$ functions derived from the crystal structures are included in Table I, and these agree very well with the values calculated from the 200 mM NaCl solution data for both oxidation states.

Discussion

In this study, the structural parameters derived from small-angle X-ray scattering have been compared for reduced and oxidized cytochrome c in "high" (200 mM NaCl) and "low" (0 mM NaCl) ionic strength solutions. The radii of gyration and maximum linear dimensions determined for the reduced form in both low and high ionic strength conditions, as well as the oxidized form at high ionic strength, are in close agreement with each other and with the parameters determined from the crystal structures. In contrast, the oxidized form at low ionic strength shows a redistribution of vectors in the $P(r)$ function such that there is a significant increase in both the radius of gyration and maximum linear dimension of the molecule.

We have considered the possibility that the X-ray scattering results could be affected by changes in the hydration layer between the two forms in the different solution conditions. Zaccai and co-workers (Zaccai et al., 1986) have found that for nonhalophilic enzymes in high-salt environments (1–4 M NaCl) the protein associates 0.2–0.3 g of water per gram of protein and negligible amounts of salt, and this causes an apparent increase in radius of gyration determined by X-ray scattering. A hydration layer of pure water can only affect the parameters determined by small-angle scattering if the mean scattering density of the bulk solvent is significantly different from the mean scattering density of pure water, thus giving rise to "contrast" between the bulk solvent, the protein, and the hydration layer. The cytochrome c measurements were done in much lower salt concentrations than was the case for the halophilic enzymes, and the difference in mean electron scattering power between 0 and 200 mM NaCl solutions is only 0.5%, compared with a difference between the mean scattering density for the protein and the bulk solvent of approximately 10%. The hydration layer is therefore not expected to contribute to the measurement of the parameters determined for the protein molecule in this case. The fact that the measured radius of gyration values and $P(r)$ functions for cytochrome c in 200 mM NaCl give such good agreement with those determined from the crystal structure coordinates supports this contention.

There are 13 lysine residues whose side chains are at the surface of cytochrome c and accessible for chemical modification (Osheroff et al., 1980). The disposition of these charged and somewhat bulky side chains might be expected to be affected by ionic strength, thus contributing to changes in R_g. Calculations of R_g were therefore done to compare the most extreme cases in which all the lysine side chains were either fully extended or folded close to the surface of the protein. The difference in the calculated R_g for these two extreme cases is only 0.2 Å. Since cytochrome c is known to have specific anion binding sites on its surface (Osherhoff et al., 1980; Taborsky & McCollum, 1979), the potential contribution to changes in R_g from preferential binding of phosphate ions to one oxidation state compared with the other has also been considered. The maximum possible contribution due to the binding of up to three phosphate ions was calculated to be less than 0.05 Å. These effects cannot, therefore, account for the increase observed in R_g on oxidation of cytochrome c at low ionic strength.

The sample preparation and solution conditions chosen for the X-ray studies were the same as those used by Eden and co-workers (Eden et al., 1982), since we were particularly interested in understanding the physical basis for the observed differences in compressibilities that these workers attributed to the change only in dynamic behavior. Kharakoz and Mkhitaryan (1986) also used these conditions for their compressibility studies. The various spectroscopic studies of hydrogen exchange rates in cytochrome c (Patel & Canuel, 1976; Ulmer & Kagi, 1968; Kagi & Ulmer, 1968; Wand et al., 1986) were done at somewhat higher ionic strengths; generally, buffered solutions between 10 and 100 mM phosphate with pH near 7 were used.

One possible explanation for the X-ray scattering results is that a part of the cytochrome c structure begins to unfold at low ionic strength and that this effect is more pronounced in the oxidized form because it carries extra net charge compared with the reduced form. A partial unfolding would give rise to an increase in radius of gyration and longer vectors in the $P(r)$ function and would also be consistent with the observations concerning the relative stabilities, as well as the different compressibilities and hydrogen exchange behavior between the oxidized and reduced forms of the protein. Cytochrome c is a highly basic protein, having a pK_i around 10.2 (Margoliash & Schejter, 1966). At pH values near 7 the protein will have a net charge of +6.6 for the reduced form or +7.1 for the oxidized form (Eden et al., 1982). In buffered

salt solutions of 100–200 mM, the counterion concentration is ample to neutralize the charge on most proteins. At significantly lower counterion concentrations, there is the potential for large electrostatic effects that could play a critical role in stabilizing the three-dimensional structure. In addition, in low ionic strength environments the motions of counterions will be coupled with those of the macromolecule, and this could affect hydrodynamic measurements, such as in the compressibility experiments.

Whether the increase in radius of gyration observed for oxidized cytochrome *c* in the low ionic strength solution environment is due to partial unfolding of the structure or some alternative rearrangement, it is clear that under the solution conditions used for the compressibility measurements there is a real structural difference between oxidized and reduced cytochrome *c*. This difference is not evident in the crystal structures because the crystals were obtained from high ionic strength solutions. The structural change observed at low ionic strength in solution is likely to be accompanied by a change in the low-frequency dynamics, and it is likely that it is a combination of changes in time-averaged structure as well as in the structural dynamics that gives rise to the different hydrogen exchange rates and apparent compressibilities between the two forms.

ACKNOWLEDGMENTS

We thank Sue Rokop for technical assistance in sample preparations. We also thank Gerald Johnson, Donald Engelman, Philip Seeger, and Murlin Nutter for assistance and technical advice in setting up the X-ray station, Peter Moore for making available the data analysis software, and Guiseppe Zaccai for his comments on the manuscript.

Registry No. Cytochrome *c*, 9007-43-6.

REFERENCES

Eden, D., Matthew, J. B., Rosa, J. J., & Richards, F. M. (1982) *Proc. Natl. Acad. Sci. U.S.A. 79*, 815.
Glatter, O. (1982) in *Small Angle X-ray Scattering* (Glatter O., & Kratky, O., Eds.) pp 119–196, Academic, New York.
Guinier, A. (1939) *Ann. Phys. (Paris) 12*, 161.
Kagi, J. H. R., & Ulmer, D. D. (1968) *Biochemistry 7*, 2718.
Kharakoz, D. P., & Mkhitaryan, A. G. (1986) *Mol. Biol. (Engl. Transl.) 20*, 312.
Kringbaum, W. R., & Kugler, F. R. (1970) *Biochemistry 9*, 1216.
Labhardt, A., & Yuen, C. (1979) *Nature (London) 227*, 150.
Margoliash, E., & Frowirth, N. (1959) *J. Biochem. (Tokyo) 71*, 570.
Margoliash, E., & Schejter, A. (1966) *Adv. Protein Chem. 21*, 113.
Moore, P. B. (1980) *J. Appl. Crystallogr. 13*, 168.
Osherhoff, N., Brautigan, D. L., & Margoliash, E. (1980) *Proc. Natl. Acad. Sci. U.S.A. 77*, 4439.
Patel, D. J., & Canuel, L. L. (1976) *Proc. Natl. Acad. Sci. U.S.A. 73*, 1398.
Taborsky, G., & McCollum, K. (1979) *J. Biol. Chem. 254*, 7069.
Takano, T., & Dickerson, R. E. (1981) *J. Mol. Biol. 153*, 95.
Ulmer, D. D., & Kagi, J. H. R. (1968) *Biochemistry 7*, 2710.
Wand, J. A., Roder, H., & Englander, S. W. (1986) *Biochemistry 25*, 1107.
Zaccai, G., & Jacrot, B. (1983) *Annu. Rev. Biophys. 12*, 139.
Zaccai, G., Wachtel, E., & Eisenberg, H. (1986) *J. Mol. Biol. 190*, 97.

A New Synthesis of Adenosine 5′-([$\gamma(R)$-^{17}O,^{18}O]-γ-Thiotriphosphate) and Its Use To Determine the Stereochemical Course of the Activation of Glutamate by Glutamine Synthetase†

Richard C. Bethell and Gordon Lowe*
Dyson Perrins Laboratory, South Parks Road, Oxford University, Oxford OX1 3QY, U.K.
Received June 29, 1987; Revised Manuscript Received September 25, 1987

ABSTRACT: A new synthetic route to adenosine 5′-([$\gamma(R)$-^{17}O,^{18}O]-γ-thiotriphosphate) is described which combines chemical methods for introducing the heavy oxygen isotopes and enzymic methods for achieving the enantiospecificity. This material was used as a substrate for the activation of glutamate catalyzed by glutamine synthetase from *Salmonella typhimurium*. Analysis of the chirality of the [^{16}O,^{17}O,^{18}O]thiophosphate produced showed that the reaction proceeds with inversion of configuration on phosphorus. This result, taken together with the positional isotope exchange studies of Midelfort and Rose [Midelfort, C. F., & Rose, I. A. (1976) *J. Biol. Chem. 251*, 5881–5887], demonstrates that the activation of glutamate to form γ-glutamyl phosphate proceeds by a direct "in-line" transfer of the phosphoryl group.

Glutamine synthetase [L-glutamate:ammonia ligase (ADP-forming), EC 6.3.1.2] catalyzes the conversion of glutamate to glutamine and is responsible for the assimilation of ammonia. Since glutamine is the biosynthetic source of nitrogen for amino acids, purines, pyrimidines, and many other molecules essential for cellular activity, its enzymic activity is regulated in a complex way by many cellular metabolites, by adenylylation and deadenylylation, and by a closed bicyclic cascade mechanism (Rhee et al., 1985). However, there are considerable differences between the glutamine synthetases from different species. The prokaryotic enzymes are usually dodecameric (Valentine et al., 1968; Shapiro & Ginsburg, 1968), while eukaryotic enzymes are octameric (Meister, 1985). The unadenylylated glutamine synthetase from *Salmonella typhimurium*, whose crystal structure was reported recently at 3.5-Å resolution (Almassey et al., 1986), is the

† This work was supported by the Science and Engineering Research Council and I.C.I. Plc, Plant Protection Division, with a CASE studentship (to R.C.B.).

0006-2960/88/0427-1125$01.50/0